Author/s:
Bennett, AC;Arndt, SK;Bennett, LT;Knauer, J;Beringer, J;Griebel, A;Hinko-Najera, N;Liddell, MJ;Metzen, D;Pendall, E;Silberstein, RP;Wardlaw, TJ;Woodgate, W;Haverd, V

Title:
Thermal optima of gross primary productivity are closely aligned with mean air temperatures across Australian wooded ecosystems

Date:
2021-10-01

Citation:
Bennett, A. C., Arndt, S. K., Bennett, L. T., Knauer, J., Beringer, J., Griebel, A., Hinko-Najera, N., Liddell, M. J., Metzen, D., Pendall, E., Silberstein, R. P., Wardlaw, T. J., Woodgate, W. & Haverd, V. (2021). Thermal optima of gross primary productivity are closely aligned with mean air temperatures across Australian wooded ecosystems. Global Change Biology, 27 (19), pp.4727-4744. https://doi.org/10.1111/gcb.15760.

MS. ALISON C. BENNETT (Orcid ID : 0000-0002-8249-976X)
DR. LAUREN T BENNETT (Orcid ID : 0000-0003-2472-062X)
MR. JÜRGEN KNAUER (Orcid ID : 0000-0002-4947-7067)
DR. ANNE GRIEBEL (Orcid ID : 0000-0002-4476-8279)
DR. ELISE PENDALL (Orcid ID : 0000-0002-1651-8969)
DR. VANESSA HAVERD (Orcid ID : 0000-0003-4359-5895)

Article type : Primary Research Article

Thermal optima of gross primary productivity are closely aligned with mean air temperatures across Australian wooded ecosystems

List of Authors:

Bennett, Alison C [1]; Arndt, Stefan K. [1]; Bennett, Lauren T. [2]; Knauer, Jürgen [3], Beringer, Jason [4], Griebel, Anne [5]; Hinko-Najera, Nina [2]; Liddell, Michael J. [6]; Metzen, Daniel [5]; Pendall, Elise [5]; Silberstein, Richard P. [4 7], Wardlaw, Timothy J. [8], Woodgate, William [9 10]; Haverd, Vanessa [3†]

Institutional Affiliations:

[1] School of Ecosystem and Forest Science, University of Melbourne, Richmond, VIC, Australia

[2] School of Ecosystem and Forest Science, University of Melbourne, Creswick, VIC, Australia

[3] CSIRO, Oceans and Atmosphere, Canberra, ACT, Australia

[4] School of Agriculture and Environment, The University of Western Australia, Crawley, 6009

[5] Hawkesbury Institute for the Environment, Western Sydney University, Penrith NSW, Australia

[6] Centre for Tropical Environmental and Sustainability Science and College of Science and Engineering, James Cook University, Cairns, QLD, Australia

[7] Centre for Ecosystem Management, School of Science, Edith Cowan University, Joondalup, WA, Australia

[8] ARC Centre for Forest Value, University of Tasmania, Hobart, TAS.

[9] CSIRO, Land and Water, Canberra, ACT, Australia

[10] School of Earth and Environmental Sciences, The University of Queensland, St Lucia, 4067, Australia

---

† Vanessa Haverd passed away in January 2021 whilst the manuscript was being prepared for initial submission. Her significant contribution to this work is vouched for by the first author.

Contact Information: bennetta2@student.unimelb.edu.au; 0439 341 344

Author contributions:

The project was conceived by VH and ACB. The analyses were conducted by ACB with guidance from VH, SKA, LTB, and contributions from JK. The manuscript was prepared by ACB with contributions from LTB, SKA, and JK. All other co-authors (JB, AG, NHN, MJL, DM, EP, RPS, TJW, WW) contributed data, site-specific interpretation, and editing of the manuscript.

Acknowledgements:

We thank the Terrestrial Ecosystem Research Network (TERN) for their support of the Australian Government National Collaborative Infrastructure Strategy (NCRIS) that provide funding to the OzFlux network. Without their support, this work would not have been possible. We also thank Peter Isaac of TERN for early discussions on flux partitioning and his insights into the effects of topography on eddy covariance observations, and Wayne Meyer for providing data and advice on the Calperum ecosystem. ACB is supported by an Australian Government Research Training Program Scholarship provided by the Australian Commonwealth Government. Additional support to co-authors comes from the Integrated Forest Ecosystem Research Program (supported by the Victorian Department of Environment, Land, Water and Planning; LTB) and the Australian Research Council DECRA Fellowship (DE190101182; WW).

Conflict of Interest:

The authors declare no conflicts of interest.

Abstract

Gross Primary Productivity (GPP) of wooded ecosystems (forests and savannas) is central to the global carbon cycle, comprising 67-75% of total global terrestrial GPP. Climate change may alter this flux by increasing the frequency of temperatures beyond the thermal optimum of GPP (T_{opt}). We examined the relationship between GPP and air temperature (Ta) in 17 wooded ecosystems dominated by a single plant functional type (broadleaf evergreen trees) occurring over a broad climatic gradient encompassing 5 ecoregions across Australia ranging from tropical in the north to Mediterranean and temperate in the south. We applied a novel boundary-line analysis to eddy covariance flux observations to a) derive ecosystem GPP-Ta relationships and T_{opt} (including seasonal analyses for 5 tropical savannas); b) quantitatively and qualitatively assess GPP-Ta relationships within and among ecoregions; c) examine the relationship between T_{opt} and mean daytime air temperature (MDTa) across all ecosystems; and d) examine how down-welling short-wave radiation (Fsd) and vapour pressure deficit (VPD) influence the GPP-Ta relationship. GPP-Ta relationships were convex parabolas with narrow curves in tropical forests, tropical savannas (wet season), and temperate forests, and wider curves in temperate woodlands, Mediterranean woodlands, and tropical savannas (dry season). Ecosystem T_{opt} ranged from 15 °C (temperate forest) to 32 °C (tropical savanna - wet and dry seasons). The shape of GPP-Ta curves was largely determined by daytime Ta range, MDTa, and maximum GPP with the upslope influenced by Fsd and the downslope influenced by VPD. Across all ecosystems, there was a strong positive linear relationship between T_{opt} and MDTa (adjusted R^2: 0.81; Slope: 1.08) with T_{opt} exceeding MDTa by >1 °C at all but two sites. We conclude that ecosystem GPP has adjusted to local MDTa within Australian broadleaf evergreen forests and that GPP is buffered against small Ta increases in the majority of these ecosystems.

Introduction

Gross Primary Productivity (GPP) of wooded ecosystems (i.e. forests and savannas) is central to the global carbon cycle because they contribute around 67-75% of the terrestrial GPP flux (Cai *et al.*, 2014), which is the largest global terrestrial carbon flux (Beer *et al.*, 2010). Air temperature (Ta) is one of the key climatic variables that determines the spatial distribution of terrestrial GPP (Anav *et al.*, 2015, Jung *et al.*, 2011). Hence, with global average surface temperatures set to increase by 1.0 to 4.0 °C by the end of the century (Collins *et al.*, 2013), it is crucial to examine relationships between Ta and GPP in wooded ecosystems. Understanding these relationships is needed to evaluate and improve Earth System models (Liu, 2020), decrease uncertainty in modelling GPP under current and future climates (Booth *et al.*, 2012), and improve knowledge of how ecosystems adjust (i.e. adapt and acclimate) to their environment (Drake *et al.*, 2015). Crucially, ecosystem-scale responses of GPP to Ta in wooded ecosystems remain largely under-examined.

Ecosystem-scale studies are needed to assess the relationship between GPP and Ta in wooded ecosystems. The leaf-level temperature dependencies of photosynthesis are well-understood; however, multiple factors contribute to differences in optimum temperature of photosynthesis (T_{opt}) between the leaf and ecosystem scale (Huang *et al.*, 2019a). For example, leaves within ecosystems are non-uniform and leaf-level photosynthesis is also affected by leaf age (Wilson *et al.*, 2000, Wilson *et al.*, 2001), leaf damage (Keith *et al.*, 2012, Kirschbaum *et al.*, 2007), leaf water status (Lawlor, 1995), nutrient availability (Longstreth & Nobel, 1980), and stomatal conductance (Leuning, 1995), each, in turn, influenced by environmental conditions. Moreover, ecosystem-scale photosynthesis is also influenced by ecosystem properties such as canopy-structure (Sprintsin *et al.*, 2012) and associated effects on leaf shading (Boardman, 1977, Valladares *et al.*, 2016), and micro-climate (De Frenne *et al.*, 2021, Nakamura *et al.*, 2017), as well as species composition (Wilson *et al.*, 2000), phenology (Keenan *et al.*, 2014) and leaf area index (LAI) (Duursma *et al.*, 2009).

As T_{opt} at leaf and ecosystem scales differ, so might the shape of the GPP-Ta relationship vary with scale and ecosystem type. At the leaf scale the shape of the relationship between the rate of net photosynthesis (A_{net}) and Ta is a convex parabolic curve whereby A_{net} increases with Ta to an optimum (T_{opt}) after which it decreases (Yamori *et al.*, 2014). In C3 species, T_{opt} ranges between 10-35 °C and the A_{net}-Ta curve is typically constrained by Ribulose bisphosphate (RuBP) and inorganic phosphate (P_i) regeneration at

low temperatures and by Rubisco activase and electron transport at high temperatures (Sage & Kubien, 2007, Yamori *et al.*, 2014). In contrast, both T_{opt} and the maximum rate of A_{net} are higher in C4 species and the A_{net}-Ta curve is likely constrained by Rubisco activity or pyruvate phosphate dikinase (PPDK) at low temperatures and electron transport or phosphoenolpyruvate (PEP) and RuBP regeneration at high temperatures (Yamori *et al.*, 2014). A_{net} is also limited by illuminance and vapour pressure deficit (VPD) (Ludlow & Wilson, 1971, Shirke & Pathre, 2004) and the T_{opt} of A_{net} is affected by the prevailing Ta during plant growth through the process of acclimation (ie. environmentally induced, non-genetic alteration of the photosynthetic mechanism; Berry & Bjorkman, 1980, Yamori *et al.*, 2014). Because GPP is the combined photosynthetic rate of all leaves within an ecosystem, we could reasonably expect the GPP-Ta relationship to take a similar parabolic form (i.e., GPP increasing with Ta to an optimum and then decreasing). Yet how the shape of the curve differs among contrasting ecosystems and how the curve is constrained at high and low Ta is largely unknown.

Cumulative evidence suggests that the shape of the GPP-Ta relationship varies considerably among ecosystems. Relationships include convex curves with a clear peak (Huang *et al.*, 2019a, Smith *et al.*, 2020), relatively flat curves that are either convex or concave (Fei *et al.*, 2018, Pau *et al.*, 2018), to roughly linear decline (Smith *et al.*, 2020, Wu *et al.*, 2017) or linear increase (Fei *et al.*, 2018, Pau *et al.*, 2018). However, these differences in shape may be attributed to variations in methodology rather than inherent differences among ecosystems. For instance, Fei *et al.* (2018) presented a relationship between daily average Ta and GPP that assumed an underlying quadratic model with data aggregation potentially excluding the high Ta range in some ecosystems. Similarly, Wu *et al.* (2017) presented a relationship between Ta and GPP normalised by a reference light use efficiency (LUE) that removed observations at low temperatures (< 25 °C). In these two studies, data aggregation and filtering limited the observational Ta range, potentially excluding T_{opt} and resulting in an apparently linear relationship. Likewise, by presenting separate relationships for morning and afternoon observations, Pau *et al.* (2018) reduced the Ta range in each period, which may also have excluded T_{opt}. Furthermore, error may be introduced by using data derived from gap-filling algorithms (e.g. Smith *et al.*, 2020) or by using MODIS NIR_v as a proxy for GPP (e.g. Huang *et al.*, 2019a) given that correlations between NIR_v and eddy-covariance flux derived GPP at the monthly timescale are not consistently high (Badgley *et al.*, 2019, Huang *et al.*, 2019b).

To our knowledge, there are no studies that have directly assessed the 'instantaneous' (i.e., half hourly to hourly) relationship of GPP with Ta across the full range of ecosystem Ta using eddy-covariance flux derived observations without assuming an underlying model form. Such studies can reveal the immediate relationship between Ta and carbon exchange across the full ecosystem Ta range (i.e., encompassing the complete range of daily and seasonal Ta). This has been demonstrated by Ma *et al.* (2017), who examined the NEP-Ta relationship in an oak-grass savanna using half-hourly eddy-covariance flux observations. By studying the GPP-Ta relationship across broad climatic-gradients we may gain further insight into the generality of the short-term GPP responses to Ta within and among a range of growing conditions at a common scale. This may lead to development of the ecosystem-scale response functions needed to improve predictability of the terrestrial carbon cycle (Luo *et al.*, 2015).

Relationships between T_{opt} of GPP and mean daytime air temperature (MDTa) can also provide information on how ecosystems have adjusted to prevailing climatic conditions. It is well-established that plants acclimate the T_{opt} of photosynthesis to growth temperature at the leaf-scale (Berry & Bjorkman, 1980, Kumarathunge *et al.*, 2019, Sage & Kubien, 2007, Vico *et al.*, 2019, Yamori *et al.*, 2014) and there is growing evidence that this also occurs at the ecosystem scale over fairly short time periods (1-14 days, Vico *et al.*, 2019). Over long time scales, there are established linear relationships between the T_{opt} of GPP and mean monthly maximum summer Ta in diverse ecosystems across North America and Europe (Baldocchi *et al.*, 2001); between the T_{opt} of GPP and mean annual maximum growing season Ta across a diversity of global biomes (Huang *et al.*, 2019a); and between the T_{opt} of GPP and mean annual Ta across evergreen needleleaf forests, deciduous broadleaf forests, and mixed deciduous and evergreen needleleaf forests globally (Niu *et al.*, 2012). These studies demonstrate adjustment of GPP to growing Ta across a broad range of ecosystems dominated by different plant functional types (PFTs) yet it remains unclear if such relationships hold across ecosystems dominated by a single PFT. Moreover, restricting the analysis to a single PFT may reduce the influence of confounding factors (i.e., phenology, physiology, canopy structure, hydraulic functioning) on the GPP-Ta relationship. The Australian continent offers a unique opportunity to address this knowledge gap because it encompasses a broad Ta range (Bennett *et al.*, 2020) and supports a diversity of wooded ecosystems dominated by a single PFT (broadleaf evergreen tree, Bonan *et al.*, 2002) mostly within a single plant family (Myrtaceae, e.g., *Eucalyptus and Corymbia spp.*).

In this paper, we examined the instantaneous GPP-Ta relationship in 17 Australian broadleaf evergreen ecosystems from five ecoregions using eddy covariance observations drawn from the OzFlux network (Beringer *et al.*, 2016). Using a unique boundary-line analysis, we isolated GPP-Ta relationships and the T_{opt} of GPP per ecosystem and examined their variation within and among ecoregions. We then examined the continent-wide relationship between the T_{opt} of GPP and the annual mean daytime Ta (MDTa) across ecosystems. We hypothesised that the shape of the instantaneous ecosystem-level GPP-Ta relationship would 1) take the form of a convex parabola with a clear T_{opt} of GPP (i.e. reflecting the shape of the A_{net}-Ta response); 2) be more similarly shaped within than among ecoregions (i.e. similar growing conditions will lead to similarly shaped curves); and that 3) there would be a positive linear relationship between the T_{opt} of GPP and MDTa across Australian wooded ecosystems (i.e. that ecosystem GPP adjusts to growing Ta).

Methods

Study sites

Our study involved 17 Australian wooded ecosystems in the TERN OzFlux network of micro-meteorological eddy covariance flux stations (Figure 1). We selected 17 of 40 potential Australian eddy covariance flux sites based on the following criteria: 1) tallest strata dominated by native woody species (tree or tall shrub); 2) no history of intensive management for agriculture nor of timber harvesting during the observation period; and 3) reliable (i.e. unaffected by significant instrument failure) eddy covariance data for more than 1 year (Table 1). The selected ecosystems encompassed a diverse range of environmental conditions including 4 major climate zones (Stern & Dahni, 2013), and 5 world ecoregions: tropical savannas (SAV); tropical forests (TRF); temperate forests (TMF); temperate woodlands (TMW); and Mediterranean woodlands (MTW) (Beringer *et al.*, 2016). None of the sites were under any form of intensive management during the study period, however several sites were subjected to disturbances from selective timber harvesting, fire-suppression, wildfire, cyclones, and insect-attack prior to (1-40 years) the study period. Across the sites, mean annual Gross Primary Productivity (GPP) ranged from 3.7 ± 0.9 (SD) t C ha^{-1} yr^{-1} to 32.1 ± 2.5 t C ha^{-1} yr^{-1}, mean annual temperature (MAT) from 9.7 ± 0.6 °C to 27.1 ± 1.0 °C, and mean annual precipitation (MAP) from 265 ± 108 mm to 4239 ± 1461 mm (Table 1).

Eddy covariance data

All sites used the eddy covariance method to measure Net Ecosystem Exchange of CO_2 (NEE) under standard data collection and curation protocols (Isaac *et al.* (2017), Table SI 1, Supplementary Methods 1). To acquire data, we first contacted all site Principal Investigators (PIs) as listed on the TERN OzFlux website (http://ozflux.org.au/monitoringsites) to identify: 1) the preferred data source for their site; and 2) any site-specific issues that may have impacted data quality for any given period. Of the 17 sites, nine opted to provide data processed to site-specific standards, and six identified periods of data to exclude (Table SI 2). We thus obtained data directly from site PI's for nine sites and downloaded data from the OzFlux OPeNDAP server (http://dat.ozflux.org.au) for the remaining eight sites. The PyFluxPro software was used at all sites to quality control and process data from raw observations as described in Isaac *et al.* (2017). Sites either used

PyFluxPro or the 'Dynamic Integrated Gap-filling and partitioning for OzFlux' (DINGO, Beringer *et al.*, 2017) software to partition NEE into the component fluxes of Ecosystem Respiration (ER) and GPP. We used GPP estimates that were partitioned from NEE using Artificial Neural Network algorithms (ANN) after confirming that there was a) strong correlation ($R^2 \geq 0.98$) between GPP estimates partitioned by the two software programs (Figure SI 1) and b) a consistent ER-Ta relationship among sites (Figure SI 2, Supplementary methods 2).

In addition to site-specific criteria provided by site PI's (Table SI 2), we filtered the data to include only paired half-hourly or hourly (TMF-Tum) Ta and GPP observations (i.e. excluding data inserted from gap-filling algorithms), derived during the daytime (shortwave downwelling radiation Fsd $\geq$ 10 W m^{-2}) where GPP $\geq$ 0 µmol $m^{-2}s^{-1}$ (i.e., removing negative GPP observations on the basis that they are implausible). All post-fire data for sites affected by wildfire during the eddy covariance record were excluded from the date of the fire to the end of the data record, except savanna ecosystems on the basis that a) fires in Australian savannas are very frequent (i.e. annual to biannual; Beringer *et al.*, 2015); b) the boundary-line analysis (see below) would minimise the influence of post-fire reduced GPP on our results; and c) savanna GPP recovers quickly (typically within 60 days) after fire (Beringer *et al.*, 2007).

Across the 17 sites there were 139.7 site years of data, with the data record ranging from 17.9 (SAV-How) to 1.4 (TMF-Wac) site years (Table 1 & Table SI 3). From the original gap-filled 2,292,814 half-hourly to hourly observations, 680,415 remained after we applied all filtering criteria. 88% of observations remained after filtering for site-specific criteria; 31% of observations remained after also filtering out night-time (Fsd $\geq$ 10 W m^{-2}) and gap-filled records; and 29.7% of the original observations remained after filtering for positive GPP (GPP $\geq$ 0 µmol $m^{-2}s^{-1}$; Table SI 3).

Boundary-Line Analysis

To test our first hypothesis, we analysed the GPP-Ta relationship using boundary-line analysis (BLA). We selected this method because multicollinearity of Ta with VPD and Fsd (Table SI 4 and Table SI 5), limited the use of standard regression techniques. BLA is less sensitive to outliers, and does not introduce circularity or bias, which can occur with alternative methods of dealing with collinearity in ecology (Dormann *et al.*, 2013). BLA thus enabled us to isolate the underlying statistical relationship between GPP and Ta at the upper

boundary of the distribution, thus minimising the effect of other variables that limit GPP (like Fsd and VPD) below the boundary (Cade & Noon, 2003). Initially proposed by Webb (1972) BLA has been used to determine the Ta optima of tree stem growth (Hinko-Najera *et al.*, 2019), tree stomatal responses to Ta (Chambers *et al.*, 1985), and the effect of forest edges on tree water relations (Wright *et al.*, 2012).

We determined the boundary line using a novel approach. BLA commonly uses the 99th quantile, however, indirectly derived GPP from flux observations is inherently noisy, with occasional GPP spikes across the full Ta range. Thus, to choose the boundary line, we placed all filtered GPP observations in 1 °C Ta bins and calculated the 50^{th} to 99^{th} quantile of GPP in increments of 5 (i.e. 50^{th}, 55^{th}, … 95^{th}, 99^{th}) for each Ta bin. We then removed all Ta bins containing <30 GPP observations per quantile to ensure adequate observation numbers. Next, we plotted GPP against Ta for each quantile, and applied Loess smoothing across bins using the "Stats" package in R (R Core Team, 2017) to preserve the natural shape of the GPP-Ta function. We then selected the boundary line as the uppermost quantile in which T_{opt} fell within 2 °C across three successive quantiles at all sites (Figure SI 3 and Figure SI 4). This was the 90^{th} quantile. We calculated T_{opt} as the Ta bin in which the smoothed GPP reached its maximum value along the 90^{th} quantile (i.e., on the boundary line, R code is supplied in Supplementary methods 3).

We also examined the influence of two important covariates, VPD and Fsd, on the derived GPP-Ta curve and T_{opt}. Firstly, we plotted the 90^{th} quantile of binned (i.e., 1 °C Ta bins at the boundary line) VPD, Fsd, and GPP observations against Ta after normalising data to the VPD, Fsd, GPP, and Ta ranges across all sites. This allowed us to examine the variation in Fsd, VPD and GPP with Ta on a common scale. Secondly, we used linear regression to examine the relationships of T_{opt} with the 50^{th} and 90^{th} quantiles of VPD and Fsd.

To test our second hypothesis, we applied both a quantitative and a qualitative approach. Firstly, for each site we quantified the shape of the GPP-Ta curve at T_{opt}. Here we defined T_{opt} as the vertex of the parabola and fitted a quadratic function at the 90^{th} quantile using the "quantreg" package in R (Koenkier, 2019, R Core Team, 2017). We then calculated the curvature (k) of the quadratic function at the vertex for each site using equation (1), where a, and b are parameter estimates of the fitted quadratic function. k indicates the direction and extent of curvature. Positive values indicate that the curve is convex, negative

values indicate that it is concave, large values indicate strong curvature (i.e. sharp curves), and small values indicate weak curvature (i.e. flat curves).

$$k = \frac{2a}{(1 + (2ax + b)^2)^{\frac{2}{3}}} \quad (1)$$

Secondly, we compared site-level normalised GPP-Ta curves to visually examine ecoregion groupings and to qualitatively assess how Ta and GPP each affected the shape of the GPP-Ta curve among sites.

Seasonal analysis of tropical savannas

Productivity in savannas is highly seasonal (Grace *et al.*, 2006) and strongly dependent upon rainfall (Kanniah *et al.*, 2013). GPP is higher during the wet season (Chen *et al.*, 2003), when annual C4 grasses contribute approximately half of ecosystem GPP, whereas in the dry season GPP is driven by perennial C3 wooded species and grass GPP is negligible (Ma *et al.*, 2020, Moore *et al.*, 2016). To isolate the response of the wooded component we analysed both the wet and dry season response of GPP to Ta for the five savanna ecosystems separately (Figure SI 4). When analysing the shape of the GPP-Ta curve between ecoregions we limited the tropical savanna data to the dry season to enable direct comparisons of broadleaved evergreen trees among ecoregions without any confounding effects of the savanna grasses.

In the Australian tropics the wet season onset date varies in space and time (Cook & Heerdegen, 2001), thus a site-specific onset date for each year was needed. We used the Australian Bureau of Meteorology's definition of the wet season as "the date when at least 50 mm of rainfall has accumulated after 1 September" (Bureau of Meteorology, 2020b), and calculated the cumulative yearly sum of precipitation from the gap-filled observations for each tropical savanna site to identify this date. The end of the wet season was defined as the first date after which no rainfall had fallen for 14 days after March 1 (i.e., the nominal end of the Australian summer). Where weather data were missing, we used 1 September for the wet-season onset date and 1 May as the end date. For the majority of sites and years, rainfall events during the period we defined as 'dry' were negligible, though occasional (<25 mm) rainfall events occurred during the dry season at all sites (for example SAV-Ade in 2007, SAV-DaS in 2009 and 2010; Figure SI 5, Table SI 6). In three years at SAV-DaS (2012, 2015, 2016) and four years at SAV-How (2004, 2005, 2013, 2016) rainfall events of 10-30 mm occurred soon after we had defined the onset of the dry season. Rather than redefine the end date, we chose to accept these as isolated events in a minority of years. All GPP

observations were assigned to either the wet or dry season and boundary-line analysis was applied to each season separately.

Relationship between T_{opt} and MDTa

To test our third hypothesis, we examined the relationship between site-level T_{opt} and MDTa. We used MDTa in preference to mean annual temperature (MAT) because photosynthesis and thus GPP are light dependent, and T_{opt} is thus likely to be more closely coupled with MDTa than MAT, which includes night-time Ta. Because wet-season GPP is equally dominated by C4 grasses in the tropical savanna sites (Ma *et al.*, 2020) we used only dry-season data and tested the strength of the T_{opt}-MDTa relationship with and without these sites. MDTa was calculated as the annual mean of daily daytime mean temperatures, which were calculated from gap-filled observations of Ta where Fsd ≥ 10 W m^{-2} and where full years of data were available (2).

$$MDTa = \frac{\sum_{i=1}^{n} Ta_i}{n} \quad (2)$$

Where n is the number of observations per year, i is the observation number (half-hourly or hourly), and Ta_i is the Ta for the i^{th} observation (°C).

Results

GPP-Ta relationship in forests and woodlands

The GPP-Ta relationship across all sites took the form of a convex parabola with the shape varying among ecoregions (Figure 2). At the temperate and tropical forest sites GPP tended to increase rapidly with Ta to a sharp vertex (T_{opt}) after which GPP declined more steeply (Figure 2 g-l). This was observed at all tropical forests and the most southerly temperate forest site (i.e., TMF-Wrr compared with TMF-Tum; TMF-Wom; and TMF-Wac). Curvature of the quadratic function at T_{opt} was highest at the most northerly tropical forest site (TRF-Ctr, k= -0.13), followed by TRF-Rob and TMF-Wrr (k=-0.06), and then the remaining temperate forest sites (TMF-Tum, TMF-Wom, TMF-Wac (k=-0.03, Table 2). In contrast, the GPP-Ta relationships at the Mediterranean woodland and temperate woodland sites were flatter, with GPP increasing gradually to T_{opt} and thereafter gradually declining (Figure 2 a-f). The curvature at T_{opt} was lowest for these sites ranging from -0.02 (MTW-Gin) to < -0.01 (MTW-GWW). At all sites VPD increased with Ta and higher VPD was associated with the downslope of the GPP-Ta curve beyond T_{opt} (Figure 3a-d, Figure SI 6). This trend was strongest at the Mediterranean (Figure 3a) and temperate (Figure 3b) woodland sites, where VPD reached the highest value among ecoregions. Fsd also increased with Ta at all sites (Figure 3a-d, Figure SI 7) and increasing Fsd was associated with the upslope of the GPP-Ta curve before T_{opt}. In the temperate (Figure 3c) and tropical (Figure 3d) forest sites the increase in Fsd with Ta corresponded closely with the GPP-Ta curve through the low temperature range before T_{opt}.

The T_{opt} range across the ecosystems was 15 °C (TMF-Wac) to 30 °C (TRF-Ctr). The range in ecosystem T_{opt} was within 1 °C in the temperate woodlands (22 °C at TMW-Cum and 23 °C at TMW-Whr) and within 2 °C in the temperate forests (15 °C at TMF-Wac to 17 °C at TMF-Tum and TMF-Wom). In contrast, the range in ecosystem T_{opt} was relatively high in the Mediterranean woodlands (5 °C range; 17 °C at MTW-Boy to 22 °C at MTW-Gin) and T_{opt} differed significantly between the two tropical forests (6 °C range; 24 °C at TRF-Rob and 30 °C at TRF-Ctr; Figure 2). T_{opt} consistently exceeded or fell within 1°C of MDTa, and was always within the daytime summer Ta range of mean daytime minimum to mean daytime maximum Ta except at TRF-Ctr where T_{opt} exceeded the mean summer daytime maximum Ta by ~ 4 °C.

GPP-Ta relationships in tropical savannas

366 The GPP-Ta relationship in tropical savannas differed in the wet and dry seasons
367 (Figure 4 a-e). The dry season GPP-Ta curves were comparatively flat, similar in appearance
368 to the Mediterranean woodland and temperate woodland curves, although curvature of the
369 quadratic function at T_{opt} ranged from -0.02 to -0.04, which was more similar to that of the
370 temperate forest sites (Table 2). The wet-season GPP-Ta curves were steeper and narrower
371 than dry season curves with curvature that ranged from -0.05 (SAV-Dry) to -0.17 (SAV-
372 Ade). The GPP peak in the wet season exceeded the peak in the dry season by between 4.9
373 μmol CO_2 m^{-2} s^{-1} (SAV-Dry) and 16.7 μmol CO_2 m^{-2} s^{-1} (SAV-Ade). The VPD range was
374 relatively uniform across the full Ta and GPP range at all savanna sites in both the wet and
375 dry seasons (Figure SI 8). Nonetheless, VPD increased almost linearly with Ta at the 90th
376 quantile in both seasons with a steeper slope that was restricted to the upper 60% of the Ta
377 range in the wet season (Figure 3e-f). Higher VPD corresponded with the downslope of the
378 GPP-Ta curve after T_{opt}. Fsd also increased with Ta in both seasons and there was a tendency
379 for lower Fsd to correspond with the upslope of the curve before T_{opt} (Figure 3e-f, Figure SI
380 9).
381 T_{opt} differed between the seasons at all tropical savanna sites. Wet-season T_{opt} was
382 within a 1 °C range across sites (32 °C at SAV-How and 31 °C at all other sites). In contrast,
383 the dry-season T_{opt} range across savanna sites was 7 °C (25 °C at SAV-Dry to 32 °C at SAV-
384 Ade). Dry-season T_{opt} was usually lower than wet-season T_{opt}, and the difference ranged from
385 3 °C (SAV-DaS, SAV-How, and SAV-Lit) to 5 °C (SAV-Dry), though SAV-Ade departed
386 from this pattern with dry-season T_{opt} 1 °C higher than wet-season T_{opt} (Figure 4 a-e).
387 Seasonal T_{opt} was always within the seasonal range in mean daytime maximum Ta
388 and mean daytime minimum Ta at the savanna sites. During the wet season T_{opt} was
389 consistently higher than both the annual MDTa (+1.4 °C at SAV-Dry to +3.1 °C at SAV-
390 How) and the seasonal MDTa (+0.1 °C at SAV-Dry to +2.6 °C at SAV-How). In contrast,
391 dry-season T_{opt} exceeded the annual MDTa at only one site (SAV-Ade; +2.6 °C) and fell
392 either below (-1.1 °C at SAV-DaS; -4.6 °C at SAV-Dry) or within 1 °C of the annual MDTa
393 (+0.1 °C at SAV-How; -0.2 °C at SAV-Lit) at the remaining sites. Dry season T_{opt} also
394 exceeded dry-season MDTa at SAV-Ade (+3.0 °C), was below dry-season MDTa at SAV-
395 Dry (-4.6 °C), and was within 1 °C at the remaining sites (-0.2 at SAV-DaS; +0.4 at SAV-Lit;
396 + 0.7 at SAV-How).
397 *The GPP-Ta relationship among ecoregions*
398 The shape of the GPP-Ta relationship was largely determined by the ecosystem GPP
399 and Ta ranges. When the GPP-Ta curves were plotted together there was strong ecoregion

grouping (Figure 5a) according to similar GPP and Ta ranges. Normalising the Ta range revealed the effect of GPP upon the shape of the curve (Figure 5b). Temperate and tropical forests grouped together with GPP at T_{opt} exceeding 24 μ mol CO_2 m^{-2} s^{-1} followed by temperate woodlands (GPP at T_{opt}: 15 to 18 μ mol CO_2 m^{-2} s^{-1}), tropical savannas (dry season; GPP at T_{opt}: 9 to 16 μ mol CO_2 m^{-2} s^{-1}) and Mediterranean woodlands (GPP at T_{opt}: 4 to 12 μ mol CO_2 m^{-2} s^{-1}). Normalising the GPP range (Figure 5c) differentiated the Mediterranean and temperate from tropical ecosystems based on the x-axis position of the curve vertex (i.e. T_{opt}), which varied from 15 to 32 °C. Normalising the ranges of both Ta and GPP (Figure 5d) caused even greater convergence of the curves, revealing that the key difference in shape among sites was the location of T_{opt} along the ecosystem Ta range. In the majority of ecosystems T_{opt} was positioned between 0.25 – 0.75 (i.e., in the mid-range of the site-level daily Ta range).

Relationship of T_{opt} with MDTa, Fsd and VPD

There was a strong positive linear relationship between T_{opt} and annual MDTa across all sites (Adjusted R^2: 0.81; Slope: 1.08, Figure 6). Removing the (dry season) tropical savanna sites weakened the strength of this relationship (Adjusted R^2: 0.66; Slope: 0.94). T_{opt} exceeded MDTa by >1 °C at all of the temperate forests, tropical forests, temperate woodlands, and one of the tropical savanna sites (SAV-Ade) varying from 1.5 °C at TMW-Cum to 6.4 °C at TMF-Tum. T_{opt} was within 1 °C of MDTa at all of the Mediterranean woodland sites and three of the tropical savannas (SAV-How; SAV-Lit; SAV-DaS); and at the remaining tropical savanna MDTa exceeded T_{opt} by 3.1 °C (Figure 6). There was a moderately strong positive relationship between T_{opt} and Fsd at the 50th quantile (Adjusted R^2: 0.61; Slope: 10.9) that was absent at the 90th quantile (Adjusted R^2: 0.05; Slope: 4.0; Figure SI 10a). In contrast, there were strong positive linear relationships of similar slope between T_{opt} and VPD at the 50th (Adjusted R^2: 0.7; Slope: 0.10) and 90th (Adjusted R^2: 0.74; Slope: 0.12) quantiles (Figure SI 10b). With the exception of tropical forests, ecoregions grouped together such that at the 90th quantile T_{opt} occurred at low VPD in temperate forests (0.9 to 1.3 kPa) compared with high VPD in tropical savannas (2.7 to 3.8 kPa).

Discussion

Examining the relationship between GPP and Ta is important for understanding how ecosystems have adjusted to historical climates and for predicting how they might respond in the future. Previous studies have demonstrated a linear relationship between growing season T_{opt} and MDTa that suggests ecosystem-scale adjustment of GPP among PFT's at the global scale (Baldocchi *et al.*, 2001, Huang *et al.*, 2019a) and we have shown that this relationship extends to ecosystems dominated by a single PFT (broadleaf evergreen trees) across a broad climatic gradient. We have also established the GPP-Ta relationship at the ecosystem scale among contrasting ecoregions, showing that the general shape of the curve (i.e., parabolic) reflects the leaf-scale thermal photosynthetic response, with strong similarities in the shape of the curve when normalised across ecosystems. However, while the leaf-scale response is governed by the rate of different photosynthetic processes at low and high Ta (Yamori *et al.*, 2014), the ecosystem scale GPP-Ta relationship is more likely to be constrained by co-varying environmental factors (i.e., Fsd and VPD) at the Ta extremes. Leaf-scale functions are incorporated within many Earth System models for simulating processes at the ecosystem scale or higher and for predicting how ecosystems may respond to future climates (Rogers *et al.*, 2017). The results of our study may serve to constrain simulated ecosystem-scale GPP-Ta responses and be used to predict the GPP-Ta relationship from relatively few ecosystem variables.

The GPP-Ta relationship is similar within ecoregions

Our boundary-line analysis revealed similar patterns in the shape of the GPP-Ta relationship within ecoregions. Consistent with our first hypothesis, the GPP-Ta relationship was a convex parabola with a discernible T_{opt} in all ecosystems that was similar in form to the leaf-level A_{net}-Ta response. Consistent with our second hypotheses, while the steepness and width of the curve and the location of T_{opt} varied among sites they were broadly similar within ecoregions. Curves were flatter with a lesser curvature and lower peak of GPP in warm/dry ecosystems with an open forest structure (woodlands and savannas) compared to wetter ecosystems with a more closed forest structure (temperate and tropical forests) where curves were steeper with a greater curvature and higher peak of GPP. While GPP in wooded ecosystems depends upon many factors other than Ta such as Fsd (Hinko-Najera *et al.*, 2017, Moore *et al.*, 2018), VPD (Griebel *et al.*, 2020, Renchon *et al.*, 2018), soil moisture (Moore *et al.*, 2018), rainfall pulses (Bartsch *et al.*, 2020), abiotic emissions (Bartsch *et al.*, 2020),

and canopy dynamics (Wu *et al.*, 2016), our results indicate that the daytime Ta range, MDTa, and ecosystem type partially explain the shape of the GPP-Ta curve. The daytime Ta range sets the overall breadth of the curve (i.e., the x-axis range) such that wider curves are associated with ecoregions that have a wide range in Ta (e.g., Mediterranean and temperate woodlands) and narrower curves are associated with ecoregions with a narrower range in Ta (e.g.., tropical forests). MDTa is associated with the x-axis position of the curve vertex at T_{opt} (on average, $T_{opt} > MDT_a$ by ~ 2 °C) such that a lower T_{opt} is associated with ecosystems from cooler climates (i.e., temperate forests) and a higher T_{opt} is associated with ecosystems from warmer climates (i.e., tropical savannas). Ecosystem type indicates the y-axis position of the curve vertex at T_{opt} by influencing the maximum rate of GPP at the boundary-line such that shallower curves are associated with ecosystems with a lower maximum (i.e., Mediterranean woodlands and tropical savannas dry-season) and steeper curves are associated with ecosystems with a higher maximum (i.e., tropical forests and temperate forests). Because ecosystem type is inextricably connected with climatic conditions, it also conveys the effect of other growth conditions that limit GPP at its peak such as water and energy limitations.

The shape of the GPP-Ta curve is also affected by environmental covariates. On the upslope of the curve before T_{opt} it is likely that Fsd is co-limiting and that this effect occurs in the low Ta range for all ecosystems in our study. Our analysis suggests that Fsd co-limitation may be important through the length of the upslope of the GPP-Ta curve in the temperate and tropical forests and the tropical savannas in the wet season. Potential explanations for this include ecosystem-scale light-limitation caused by seasonal cloud-cover in tropical ecosystems (Kanniah *et al.*, 2010, Malhi *et al.*, 2017), decreased light availability during winter (i.e. during lower Ta conditions) in southern latitudes (Hatzianastassiou *et al.*, 2005) where temperate forests grow, and the effect of forest microclimates limiting light-availability to lower canopy leaves (De Frenne *et al.*, 2021). However, the lack of a relationship between Fsd and T_{opt} (Figure SI 10a) at the 90th quantile suggests that light-limitation does not drive the position of T_{opt} on the GPP-Ta curve. On the downslope of the GPP-Ta curve, after T_{opt}, it is likely that VPD co-limitation becomes important and that this effect is stronger for the Mediterranean and temperate woodlands and the tropical savannas in the dry season. The likely explanation is a limitation to leaf-level photosynthesis driven by stomatal closure (Farquhar & Sharkey, 1982). However, the magnitude of the VPD influence on the GPP-Ta curve may be ecosystem dependent. Water availability has been shown to moderate stomatal closure under high VPD at TMF-Wom (Griebel *et al.*, 2020) and

the strong positive linear relationship between VPD and T_{opt} (Figure SI 10b) indicates tolerance to higher VPD in warmer ecoregions.

There is mixed agreement between the parabola-like GPP-Ta curves that we present and previous studies, and we suggest methodology may explain contrasting results. Our results agree most strongly with Huang *et al.* (2019a) who presented a narrow convex parabolic curve for a sample ecosystem from their global study. Several of the ecosystems presented by Smith *et al.* (2020) are of an apparently similar parabolic shape, however minimal data in the low Ta range, likely caused by averaging data at the daily timescale, frequently omitted the upslope of the curve. Our results appear to contrast with Fei *et al.* (2018) who presented curves of different form for three forested ecosystems and a savanna in Southwest China. However, they assumed a quadratic model (as opposed to our boundary line analysis), aggregated data at the daily timescale (i.e. reducing observational Ta range), and did not separate the savanna data seasonally (i.e. including wooded and grassy components in a single relationship). Our results also contrast with Wu *et al.* (2017), yet this most likely stems from a limited Ta range below T_{opt} in their study (i.e., they only show the downslope of the curve). Finally, our results partially contradict the analysis of Duffy *et al.* (2021) whose global study showed a similar parabolic shape of the GPP-Ta relationship in C3 ecosystems, yet with a common T_{opt} across all ecosystems of 18 °C. The Duffy et al. (2021) study appears to contradict previous findings of T_{opt} increasing with Ta (Baldocchi *et al.*, 2001, Huang *et al.*, 2019a, Niu *et al.*, 2012) and is lower than the previously established global average T_{opt} of 23 ±6 °C (Huang *et al.*, 2019a). Approaches to examining GPP-Ta relationships vary according to scale and data availability, and it is beyond the scope of this study to review the relative merits. Nonetheless, with some limitations (see below) we can recommend boundary-line analysis as a robust approach to assessing ecosystem-scale T_{opt} of GPP due to its ability to derive the underlying GPP-Ta relationship and retain the full ecosystem Ta range.

The GPP-Ta relationship is highly seasonal in tropical savannas

We observed large seasonal differences in the shape of the GPP-Ta relationship in tropical savannas that likely reflect seasonal shifts in the dominant vegetation. Australian savannas comprise an overstorey of predominantly eucalypt trees with an understorey of annual C4 grasses that are only active during the wet season (Beringer *et al.*, 2011). Thus, grasses and trees contribute to wet-season GPP and only trees contribute to dry-season GPP

(Ma *et al.*, 2020, Moore *et al.*, 2018, Moore *et al.*, 2016) and the shifting GPP-Ta relationship reflects this change. The higher peak of GPP and T_{opt} in the wet season may be attributed to the overall increase in photosynthetic activity (i.e., combined photosynthesis of C3 trees and C4 grasses), a higher T_{opt} of C4 photosynthesis (Yamori *et al.*, 2014); and photosynthetic adjustment (i.e., acclimation and adaptation) of plants to the prevailing Ta. The lower peak of GPP during the dry season may also be caused by changes in tree phenology and environmental conditions. For instance, canopy LAI decreases in many species during the dry season (Moore *et al.*, 2017, Whitley *et al.*, 2011, Williams *et al.*, 1997), levels of solar radiation are affected by both decreased cloud cover and increased atmospheric aerosols from fire-related activity (Kanniah *et al.*, 2010), and there are significant decreases in rainfall that affect soil moisture. Cumulatively, these changes will contribute to the seasonal differences in the upper boundary of the GPP-Ta relationship.

Seasonal shifts in T_{opt} in the tropical savannas are likely to reflect the T_{opt} for tree species during the dry season and a combination of tree and grass species during the wet season. Dry-season T_{opt} occurred close to annual MDTa, implying that perennial tree species are adapted to the average annual conditions with the exception of SAV-Ade, where the short (< 2 yr) observation period may have influenced results. Conversely, wet-season T_{opt} was close to the wet-season mean daily maximum Ta implying that grass species are more adapted to the higher wet-season Ta and potentially reflecting the higher T_{opt} of C4 photosynthesis (Yamori *et al.*, 2014). Our analysis is consistent with Ma *et al.* (2017) who examined a Californian oak-grass savanna, and identified that T_{opt} of understory grasses was ~ 2 °C lower than the oak canopy and that T_{opt} occurred between MAT and average maximum Ta. While their analysis used the net carbon flux (i.e., NEP) rather than GPP to represent ecosystem photosynthesis and they did not separate data seasonally, our studies both demonstrate that the GPP-Ta relationship of different PFTs growing at the same location can differ. Our results are also consistent with Huang *et al.* (2019a) who reported a T_{opt} of 31.2 °C for SAV-How for the growing season which is within 1 °C of our wet-season T_{opt} (32 °C) for this site.

GPP adjustment to Ta across ecosystems

Consistent with our third hypothesis, there was a strong linear relationship between T_{opt} and annual MDTa that implies the ecosystems in our study have adjusted their GPP to the prevailing Ta regime. The slope and strength of the relationship was similar to

relationships between monthly T_{opt} and mean summer Ta in North American and European ecosystems (Baldocchi *et al.*, 2001, R2: 0.83; slope: 0.93), and marginally stronger than that between the mean annual daily maximum Ta of the growing season and mean ecosystem T_{opt} across a broad array of ecosystem groups globally (Huang *et al.*, 2019a, Slope: 0.76). These previous studies demonstrated that GPP adjustment occurs across ecosystems comprised of plants from diverse PFTs and our study extends that knowledge by showing this process also occurs across ecosystems dominated by plants from a single PFT (the majority from a single family). While our results cannot distinguish adaptation (long-term genetic response) from acclimation (short-term physiological response), they add evidence that the adjustment of GPP to Ta is an inherent feature of ecosystems.

The majority of sites in our study (n=9) were operating at Ta >1 °C below their thermal optima. In temperate woodlands, temperate forests, tropical forests, and tropical savannas in the wet season the T_{opt} of GPP exceeded MDTa by ~1.5 °C or more. The remaining sites were operating at Ta within 1 °C of their thermal optima, with the exception of SAV-Dry. This has potential implications for the effect of increasing Ta on GPP under climate change as it implies that small increases in Ta would have a limited or small positive effect on GPP at the temperate woodlands, temperate forests, tropical forests and tropical savannas during the wet-season. However, Mediterranean woodlands and tropical savannas during the dry season may be more susceptible to negative impacts upon GPP, notwithstanding the effects of CO_2 fertilisation (Schimel *et al.*, 2015), thermal acclimation of photosynthesis (Way, 2019), and assuming that VPD-Fsd-Ta interactions remain similar under changing climates. These results are particularly important for tropical forests because it has been suggested that they are operating near their thermal optima (Huang *et al.*, 2019a, Pau *et al.*, 2018), or already exceeding their photosynthetic Ta optima (Mau *et al.*, 2018) and are particularly sensitive to increasing Ta (Doughty & Goulden, 2008). In contrast to these prior studies, the T_{opt} of our two tropical forest sites exceeded MDTa by +2.7 °C suggesting that GPP in these two Australian tropical forests will be sustained despite increases in Ta even under the most extreme climate change scenario (RCP8.5, Collins *et al.*, 2013). The difference in our conclusion, that tropical forests are not operating near or exceeding their T_{opt}, may be attributed to source data from Australian tropical forests being excluded from the global analysis (Huang *et al.*, 2019a) and the focus of other studies on Central and South America (Doughty & Goulden, 2008, Mau *et al.*, 2018, Pau *et al.*, 2018). Our study thus highlights the importance of studying a diversity of global forests and ensuring that a

representative sample of forests are included when projecting data across large geographic scales.

Limitations of the study

We acknowledge several limitations in our approach to examining the GPP-Ta relationship. First, the BLA technique revealed the GPP-Ta relationship when GPP was unconstrained by other factors. However, terrestrial ecosystems are often limited by available water, solar radiation (Churkina & Running, 1998, Nemani *et al.*, 2003), nutrients (Vitousek *et al.*, 2010), and the impacts of disturbance (Cooper *et al.*, 2017, Flower & Gonzalez-Meler, 2015). If ecosystems are limited by something other than Ta, the GPP-Ta relationship presented here may not often be observed in nature. Furthermore, while we expect a causal relationship between GPP and Ta, the method cannot conclusively demonstrate causality and our study indicates that the GPP-Ta curve may have been constrained by Fsd and VPD on either-side of T_{opt} at some sites (Figure 3, Figure SI 6-9). It is therefore possible that collinearity influenced our analysis, and thus the shape of the GPP-Ta curve, at the Ta extremes. In particular, we may not have fully separated the effects of Ta on GPP from those of VPD because of strong covariation at the majority of sites (Table SI 4 & Table SI 5) and because both VPD and Ta influence the rate of leaf photosynthesis (Ludlow & Wilson, 1971). VPD affects stomatal conductance, which in turn regulates the availability of CO_2 inside the leaf (Farquhar & Sharkey, 1982) and Ta affects the rate of several photosynthetic processes (Sage & Kubien, 2007). Experimental manipulation of VPD and Ta in a tropical forest mesocosm suggests that the apparent decline in GPP above T_{opt} is driven by responses to VPD rather than Ta (Smith *et al.*, 2020). Thus, a similar response may have occurred within the ecosystems in our study and there is some indication that this was the case in the Mediterranean woodlands we studied (Figure SI 6).

Third, GPP was not directly measured by the eddy covariance method (Reichstein *et al.*, 2005), rather it was partitioned from NEE using an algorithm that models the relationship between night-time ER, Ta, soil temperature, soil water content, and the greenness index (EVI) to predict daytime ER (Beringer *et al.*, 2017, Isaac *et al.*, 2017). Consequently, predictions of GPP were in some cases (< 3%) made outside the measured Ta range, and whilst we selected the GPP partitioning method that was least dependent upon Ta as an input (i.e. ANN), our analysis of the GPP-Ta relationship was not wholly independent of the GPP partitioning method. Fourth, the length of the data record varied among sites and our analysis

captured the mean relationship across those periods, the curves may thus be less representative in ecosystems with a shorter data record (e.g. SAV-Ade and TMF-Wac). The analytic method also lacked the sensitivity to capture seasonal (except in the tropical savanna sites), interannual, or decadal variations in the GPP-Ta relationship. Annual shifts in the T_{opt} of NEE have been demonstrated (Niu *et al.*, 2012), thus the T_{opt} we presented may not accurately depict current T_{opt}. Finally, Ta is different from both leaf (Dong *et al.*, 2017, Helliker & Richter, 2008, Song *et al.*, 2011) and canopy temperatures (Tcanopy, Pau *et al.*, 2018) and T_{canopy} can vary across vertical and horizontal profiles (Anhuf & Rollenbeck, 2001). Ta measurements in our study were taken above the canopy (Table SI 1), thus they may not accurately represent temperatures at the leaf-level. This limitation may be more critical at tropical sites where it has been established that T_{canopy} exceeds Ta and is more tightly coupled to GPP (Pau *et al.*, 2018) compared to temperate eucalypt sites where T_{canopy} has been shown to be within 2 °C of Ta (Woodgate *et al.*, 2020).

Overall, our study demonstrates parabola-like GPP-Ta relationships in Australia's wooded ecosystems that are similar within ecoregions and that shift seasonally in tropical savannas. The shape of the GPP-Ta relationship is closely linked to ecosystem type, the annual daytime Ta range, and MDTa such that steep narrow curves with high curvature and T_{opt} are associated with tropical forests and relatively flat, wide curves with low curvature and T_{opt} are associated with temperate woodlands. There was a strong positive linear relationship between the T_{opt} of GPP and MDTa across these 17 wooded ecosystems that conforms with global relationships. This provides further evidence that plant communities have adjusted GPP to the prevailing Ta regimes at the ecosystem scale and that this process occurs not only among ecosystem types but within those dominated by a single PFT. Our results strongly support the presence of underlying convex GPP-Ta relationships among ecosystems that are determined by relatively few ecosystem characteristics. Given the broad climatic range our study encompassed we expect this relationship to extend to other wooded ecosystems globally. We suggest future research to examine this question, as it may be possible to predict the ecosystem-scale GPP-Ta curve from the daytime Ta range, MDTa, and the maximum ecosystem GPP. The results of our study may thus potentially be used to develop ecosystem-scale response functions that are needed to improve the predictability of terrestrial earth system models. Further research should also examine how thermal acclimation of photosynthesis affects the GPP-Ta curve as this will be critical to understanding the response of the ecosystem-scale GPP-Ta relationship under climate change.

Tables

Table 1 Characteristics of the 17 OzFlux study sites ordered by increasing magnitude of annual GPP. World ecoregion reproduced from Beringer *et al.* (2016), forest type and site co-ordinates obtained from TERN OzFlux (2020), and observation period is the time period used in the study. All other values were calculated from gap-filled eddy covariance observations prior to application of filtering steps detailed in the methods section. These data were first filtered to remove incomplete calendar years. Values in parenthesis indicate the standard deviation of the mean.

World ecoregion	Tower name	Location	Forest type	Dominant species	Lat.	Long.	Observation period		GPP (t C ha^{-1} yr^{-1})	MAT (°C) mean (SD)	MAP (mm)
Mediterranean woodlands	MTW-GWW	Great Western Woodlands	Temperate woodland, shrubland and mallee	*Eucalyptus salmonophloia*	-30.19	120.65	1/01/2013	9/07/2019	3.72 (0.87)	19.5 (0.53)	337 (101)
	MTW-Cpr	Calperum	Mallee woodland	*E. dumosa, E. incrassenta, E. oleosa, E. socialis*	-34.00	140.59	30/07/2010	17/1/2014	4.24 (1.82)	18.1 (0.51)	265 (108)
	MTW-Boy	Boyagin	Wandoo woodland	*E. wandoo*	-32.48	116.94	4/12/2017	15/04/2020	8.57 (0.46)	16.3 (0.49)	388 (87)
	MTW-Gin	Gingin	Coastal heath banksia woodland	*Banksia menziessi; B. attenuate; B. grandis*	-31.38	115.71	13/10/2011	14/10/2016	11.83 (1.60)	18.3 (1.17)	669 (94)
Temperate woodlands	TMW-Cum	Cumberland Plain	Dry sclerophyll woodland	*E. moluccana; E. fibrosa*	-33.62	150.72	1/01/2014	1/01/2020	15.89 (2.46)	18.5 (0.36)	855 (227)
	TMW-Whr	Whroo	Box woodland	*E. macrocarpa; E. leucoxylon*	-36.67	145.03	1/12/2011	16/11/2019	14.28 (2.79)	15.6 (0.32)	370 (122)
Tropical savannas	SAV-Dry	Dry River	Open forest savanna	*E. tetrodonta, E. dichromophloia, C. terminalis, Sorghum intrans, S.*	-15.26	132.37	3/09/2008	1/08/2019	11.83 (0.86) *dry* 4.55 (1.20)	27.1 (0.99) 25.3 (1.2)	724 (244) 37 (19)

				plumosum, Themeda triandra,					*wet*	7.28 (0.57)	28.7 (1.0)	687 (238)
	SAV-Ade	Adelaide River	Savanna	*E. tectifica* *Planchonia careya*	-13.08	131.12	17/10/2007	23/05/2009	*dry*	18.63 (3.79) 4.91 (0.99)	26.8 (0.2) 25.9 (0.3)	1857 (111) 54 (20)
									wet	13.72 (4.91)	27.6 (0.0)	1803 (131)
	SAV-Lit	Litchfield	Tropical savanna	*E. tetrodonta, E. miniate,* *Erythrophleum chlorostachys*	-13.18	130.80	23/06/2015	8/08/2019	*dry*	16.11 (0.95) 4.40 (0.75)	26.4 (0.19) 25.5 (0.2)	1538 (384) 43 (4)
									wet	11.71 (1.64)	27.1 (0.2)	1495 (386)
	SAV-DaS	Daly Uncleared	Woodland savanna	*E. tetrodonta, C. latifolia,* *Terminalia grandifolia, Sorghum sp. Heteropogon triticeus*	-14.16	131.39	1/01/2008	4/02/2019	*dry*	15.00 (1.79) 5.13 (0.75)	26.8 (0.52) 25.7 (0.5)	1263 (206) 53 (34)
									wet	9.87 (1.69)	27.9 (0.5)	1210 (197)
	SAV-How	Howard Springs	Tropical savanna	*E.miniate* *E.tentrodonata*	-12.50	131.15	1/01/2002	8/08/2019	*dry*	21.74 (1.27) 7.44 (1.13)	26.8 (0.54) 25.8 (1.0)	1526 (318) 58 (45)
									wet	14.30 (1.74)	27.6 (0.3)	1468 (326)
World Eco Region	**Tower name**	**Location**	**Forest type**	**Dominant species**	**Lat.**	**Long.**	**Observation period**			**GPP (t C ha^{-1} yr^{-1}) mean (SD)**	**MAT (°C) mean (SD)**	**MAP (mm) mean (SD)**
Temperate forests	TMF-Wac	Wallaby Creek	Wet sclerophyll forest	*E.regnans*	-37.43	145.19	25/08/2005	31/12/2006		20.25 (NA)	10.6 (NA)	1571 (1098)
	TMF-Wrr	Warra	Wet sclerophyll forest	*E.obliqua*	-43.10	146.65	5/03/2013	1/1/2018		21.58 (0.97)	10.6 (0.43)	1340 (248)
	TMF-Wom	Wombat State Forest	Dry sclerophyll forest	*E.obliqua* *E.rubida*	-37.42	144.09	20/01/2010	20/01/2020		25.44 (2.34)	11.3 (0.34)	859 (203)
	TMF-Tum	Tumbarumba	Wet sclerophyll forest	*E.delegatensis*	-35.66	148.15	23/02/2001 1/4/2004	31/12/2001 31/12/2013		25.71 (3.60)	9.7 (0.65)	1081 (279)
Tropical forests	TRF-Rob	Robson Creek	Complex	*NA*	-17.12	145.63	1/08/2013	26/08/201		23.24 (1.32)	19.6 (0.48)	2013 (927)

			mesophyll vine forest						9			
	TRF-Ctr	Cape Tribulation	Complex mesophyll vine forest	*NA*	-16.10	145.45	1/01/2010	2/11/2018	32.14 (2.47)	24.1 (0.41)	4239 (1461)	

663

664

665 **Table 2** Parameter estimates and curvature at T_{opt} for the quadratic function fitted at the 90th
666 quantile for the 17 wooded ecosystems. T_{opt} and GPP are the *x* and *y* values of the curve
667 vertex; *a*, *b*, and *c* are parameter estimates of the quadratic function; and *k* denotes curvature
668 calculated using equation (2). The table is sorted in order of greatest to lowest curvature (the
669 negative sign denotes convex curvature) with tropical savanna sites listed separately due to
670 the segregation of data into dry and wet seasons.

Tower name	**T_{opt} (°C)**	**GPP at T_{opt} (μ mol CO_2 m^{-2} s^{-1})**	***a***	***b***	***c***	***k***
Tropical forests, temperate forests, Mediterranean woodlands, and temperate woodlands						
TRF-Ctr	30.5	38.4	-0.192	11.706	-140.188	-0.13
TMF-Wrr	17.1	29.6	-0.090	3.062	3.438	-0.06
TRF-Rob	24.2	25.4	-0.097	4.674	-31.086	-0.06
TMF-Tum	17.9	30.6	-0.049	1.758	14.820	-0.03
TMF-Wac	14.7	23.8	-0.040	1.171	15.156	-0.03
TMF-Wom	19.5	27.3	-0.039	1.539	12.200	-0.03
MTW-Gin	21.7	11.5	-0.024	1.028	0.366	-0.02
MTW-Boy	17.1	9.8	-0.020	0.685	3.982	-0.01
MTW-Cpr	21.4	7.1	-0.013	0.538	1.369	-0.01
TMW-Cum	20.4	17.6	-0.020	0.822	9.219	-0.01
TMW-Whr	23.3	15.3	-0.022	0.999	3.703	-0.01
MTW-GWW	20.5	4.5	-0.006	0.232	2.119	<0.01
Tropical savannas						
SAV-Ade	31.3	25.8	-0.252	15.766	-220.864	-0.17
SAV-How	32.4	28.2	-0.203	13.177	-185.353	-0.14
SAV-Lit	30.2	19.9	-0.185	11.143	-148.219	-0.12
SAV-DaS	30.1	22.1	-0.171	10.342	-133.857	-0.11
SAV-Dry	29.7	15.8	-0.081	4.794	-55.253	-0.05
SAV-How	30.3	15.7	-0.053	3.203	-32.839	-0.04
SAV-Dry	24.4	10.8	-0.043	2.107	-14.846	-0.03
SAV-Lit	27.0	10.5	-0.049	2.636	-25.187	-0.03
SAV-Ade	32.2	9.4	-0.034	2.182	-25.837	-0.02
SAV-DaS	27.0	10.8	-0.030	1.646	-11.424	-0.02

wet

dry

671
672

References

Anav A, Friedlingstein P, Beer C *et al.* (2015) Spatiotemporal patterns of terrestrial gross primary production: A review. Reviews of Geophysics, 53(3), 785-818. https://doi.org/10.1002/2015rg000483

Anhuf D, Rollenbeck R (2001) Canopy structure of the Rio Surumoni rain forest (Venezuela) and its influence on microclimate. Ecotropica, 7(1-2), 21-32.

Badgley G, Anderegg LDL, Berry JA, Field CB (2019) Terrestrial gross primary production: Using NIRV to scale from site to globe. Global Change Biology, 25(11), 3731-3740. https://doi.org/10.1111/gcb.14729

Baldocchi D, Falge E, Gu LH *et al.* (2001) FLUXNET: A new tool to study the temporal and spatial variability of ecosystem-scale carbon dioxide, water vapor, and energy flux densities. Bulletin of the American Meteorological Society, 82(11), 2415-2434. https://doi.org/10.1175/1520-0477(2001)082<2415:fantts>2.3.co;2

Bartsch S, Stegehuis AI, Boissard C *et al.* (2020) Impact of precipitation, air temperature and abiotic emissions on gross primary production in Mediterranean ecosystems in Europe. European Journal of Forest Research, 139(1), 111-126. https://doi.org/10.1007/s10342-019-01246-7

Beer C, Reichstein M, Tomelleri E *et al.* (2010) Terrestrial gross carbon dioxide uptake: Global distribution and covariation with climate. Science, 329(5993), 834-838. https://doi.org/10.1126/science.1184984

Bennett AC, Penman TD, Arndt SK, Roxburgh SH, Bennett LT (2020) Climate more important than soils for predicting forest biomass at the continental scale. Ecography, 43, 1-14. https://doi.org/10.1111/ecog.05180

Beringer J, Hacker J, Hutley LB *et al.* (2011) Special-savanna patterns of energy and carbon integrated across the landscape. Bulletin of the American Meteorological Society, 92(11), 1467-1485. https://doi.org/10.1175/2011bams2948.1

Beringer J, Hutley LB, Abramson D *et al.* (2015) Fire in Australian savannas: from leaf to landscape. Global Change Biology, 21(1), 62-81. https://doi.org/10.1111/gcb.12686

Beringer J, Hutley LB, Mchugh I *et al.* (2016) An introduction to the Australian and New Zealand flux tower network - OzFlux. Biogeosciences, 13(21), 5895-5916. https://doi.org/10.5194/bg-13-5895-2016

Beringer J, Hutley LB, Tapper NJ, Cernusak LA (2007) Savanna fires and their impact on net ecosystem productivity in North Australia. Global Change Biology, 13(5), 990-1004. https://doi.org/10.1111/j.1365-2486.2007.01334.x

Beringer J, Mchugh I, Hutley LB, Isaac P, Kljun N (2017) Technical note: Dynamic INtegrated Gap-filling and partitioning for OzFlux (DINGO). Biogeosciences, 14(6), 1457-1460. https://doi.org/10.5194/bg-14-1457-2017

Berry J, Bjorkman O (1980) Photosynthetic response and adaptation to temperature in higher-plants. Annual Review of Plant Physiology and Plant Molecular Biology, 31, 491-543. https://doi.org/10.1146/annurev.pp.31.060180.002423

Boardman NK (1977) Comparative photosynthesis of sun and shade plants. Annual Review of Plant Physiology and Plant Molecular Biology, 28, 355-377. https://doi.org/10.1146/annurev.pp.28.060177.002035

Bonan GB, Levis S, Kergoat L, Oleson KW (2002) Landscapes as patches of plant functional types: An integrating concept for climate and ecosystem models. Global Biogeochemical Cycles, 16(2), 1021. https://doi.org/10.1029/2000gb001360

Booth BBB, Jones CD, Collins M *et al.* (2012) High sensitivity of future global warming to land carbon cycle processes. Environmental Research Letters, 7(2), 1-8. https://doi.org/10.1088/1748-9326/7/2/024002

Bureau of Meteorology (2020, 16 March) *Climate classification of Australia*. Australian Government Bureau of Meteorology. http://www.bom.gov.au/jsp/ncc/climate_averages/climate-classifications/index.jsp?maptype=kpngrp#maps,

Bureau of Meteorology (2020, 3 March) *Northern rainfall onset*. Australian Government Bureau of Meteorology. http://www.bom.gov.au/climate/rainfall-onset/

Cade BS, Noon BR (2003) A gentle introduction to quantile regression for ecologists. Frontiers in Ecology and the Environment, 1(8), 412-420. https://doi.org/10.2307/3868138

Cai WW, Yuan WP, Liang SL *et al.* (2014) Large differences in terrestrial vegetation production derived from satellite-based light use efficiency models. Remote Sensing, 6(9), 8945-8965. https://doi.org/10.3390/rs6098945

Chambers JL, Hinckley TM, Cox GS, Metcalf CL, Aslin RG (1985) Boundary-line analysis and models of leaf conductance for 4 oak-hickory forest species. Forest Science, 31(2), 437-450.

Chen XY, Hutley LB, Eamus D (2003) Carbon balance of a tropical savanna of northern Australia. Oecologia, 137(3), 405-416. https://doi.org/10.1007/s00442-003-1358-5

Churkina G, Running SW (1998) Contrasting climatic controls on the estimated productivity of global terrestrial biomes. Ecosystems, 1(2), 206-215. https://doi.org/10.1007/s100219900016

Collins M, Knutti R, Arblaster J *et al.* (2013) Long-term climate change: Projections, commitments and irreversibility. In: *Climate change 2013: The physical science basis. Contribution of working group I to the fifth assessment report of the Intergovernmental Panel on Climate Change.* (ed Stocker TF, D. Qin, G.-K. Plattner, M. Tignor, S.K. Allen, J. Boschung, A. Nauels, Y. Xia, V. Bex and P.M. Midgley) pp 1029-1136. Cambridge, United Kingdom and New York, NY, USA, Cambridge University Press.

Cook GD, Heerdegen RG (2001) Spatial variation in the duration of the rainy season in monsoonal Australia. International Journal of Climatology, 21(14), 1723-1732. https://doi.org/10.1002/joc.704

Cooper LA, Ballantyne AP, Holden ZA, Landguth EL (2017) Disturbance impacts on land surface temperature and gross primary productivity in the western United States. Journal of Geophysical Research-Biogeosciences, 122(4), 930-946. https://doi.org/10.1002/2016jg003622

De Frenne P, Lenoir J, Luoto M *et al.* (2021) Forest microclimates and climate change: Importance, drivers and future research agenda. Global Change Biology, 27(11), 2279-2297. https://doi.org/10.1111/gcb.15569

Department of Agriculture WaTE (2019, 2 November) *Interim Biogeographic Regionalisation for Australia v. 7 (IBRA) [ESRI shapefile]*. Commonwealth of Australia. http://www.environment.gov.au/fed/catalog/search/resource/details.page?uuid=%7B4A2321F0-DD57-454E-BE34-6FD4BDE64703%7D

Dong N, Prentice IC, Harrison SP, Song QH, Zhang YP (2017) Biophysical homoeostasis of leaf temperature: A neglected process for vegetation and land-surface modelling. Global Ecology and Biogeography, 26(9), 998-1007. https://doi.org/10.1111/geb.12614

Dormann CF, Elith J, Bacher S *et al.* (2013) Collinearity: A review of methods to deal with it and a simulation study evaluating their performance. Ecography, 36(1), 27-46. https://doi.org/10.1111/j.1600-0587.2012.07348.x

Doughty CE, Goulden ML (2008) Are tropical forests near a high temperature threshold? Journal of Geophysical Research-Biogeosciences, 113, G00B07. https://doi.org/10.1029/2007jg000632

Drake JE, Aspinwall MJ, Pfautsch S *et al.* (2015) The capacity to cope with climate warming declines from temperate to tropical latitudes in two widely distributed *Eucalyptus* species. Global Change Biology, 21(1), 459-472. https://doi.org/10.1111/gcb.12729

Duffy KA, Schwalm CR, Arcus VL, Koch GW, Liang LL, Schipper LA (2021) How close are we to the temperature tipping point of the terrestrial biosphere? Science Advances, 7(3), eaay1052. https://doi.org/10.1126/sciadv.aay1052

Duursma RA, Kolari P, Peramaki M *et al.* (2009) Contributions of climate, leaf area index and leaf physiology to variation in gross primary production of six coniferous forests across Europe: A model-based analysis. Tree Physiology, 29(5), 621-639. https://doi.org/10.1093/treephys/tpp010

Farquhar GD, Sharkey TD (1982) Stomatal conductance and photosynthesis. Annual Review of Plant Physiology, 33(1), 317-345. https://doi.org/10.1146/annurev.pp.33.060182.001533

Fei XH, Song QH, Zhang YP *et al.* (2018) Carbon exchanges and their responses to temperature and precipitation in forest ecosystems in Yunnan, Southwest China. Science of the Total Environment, 616, 824-840. https://doi.org/10.1016/j.scitotenv.2017.10.239

Flower CE, Gonzalez-Meler MA (2015) Responses of temperate forest productivity to insect and pathogen disturbances. In: *Annual Review of Plant Biology, Vol 66.* (ed Merchant SS) pp 547-569. Palo Alto, Annual Reviews. https://doi.org/10.1146/annurev-arplant-043014-115540

Grace J, José JS, Meir P, Miranda HS, Montes RA (2006) Productivity and carbon fluxes of tropical savannas. Journal of Biogeography, 33(3), 387-400. https://doi.org/10.1111/j.1365-2699.2005.01448.x

Griebel A, Bennett LT, Metzen D, Pendall E, Lane PNJ, Arndt SK (2020) Trading water for carbon: Maintaining photosynthesis at the cost of increased water loss during high temperatures in a temperate forest. Journal of Geophysical Research: Biogeosciences, 125(1), e2019JG005239. https://doi.org/10.1029/2019JG005239

Hatzianastassiou N, Matsoukas C, Fotiadi A, Pavlakis KG, Drakakis E, Hatzidimitriou D, Vardavas I (2005) Global distribution of Earth's surface shortwave radiation budget.

Atmospheric Chemistry and Physics, 5, 2847-2867. https://doi.org/10.5194/acp-5-2847-2005

Helliker BR, Richter SL (2008) Subtropical to boreal convergence of tree-leaf temperatures. Nature, 454(7203), 511-U516. https://doi.org/10.1038/nature07031

Hinko-Najera N, Isaac P, Beringer J *et al.* (2017) Net ecosystem carbon exchange of a dry temperate eucalypt forest. Biogeosciences, 14(16), 3781-3800. https://doi.org/10.5194/bg-14-3781-2017

Hinko-Najera N, Umana JCN, Smith MG, Low M, Griebel A, Bennett LT (2019) Relationships of intra-annual stem growth with climate indicate distinct growth niches for two co-occurring temperate eucalypts. Science of the Total Environment, 690, 991-1004. https://doi.org/10.1016/j.scitotenv.2019.07.024

Huang MT, Piao SL, Ciais P *et al.* (2019a) Air temperature optima of vegetation productivity across global biomes. Nature Ecology & Evolution, 3(5), 772-779. https://doi.org/10.1038/s41559-019-0838-x

Huang XJ, Xiao JF, Ma MG (2019b) Evaluating the performance of satellite-derived vegetation indices for estimating gross primary productivity using FLUXNET observations across the globe. Remote Sensing, 11(15), 22. https://doi.org/10.3390/rs11151823

Isaac PR, Cleverly J, Mchugh I, Van Gorsel E, Ewenz C, Beringer J (2017) OzFlux data: Network integration from collection to curation. Biogeosciences, 14(12), 2903-2928. https://doi.org/10.5194/bg-14-2903-2017

Jung M, Reichstein M, Margolis HA *et al.* (2011) Global patterns of land-atmosphere fluxes of carbon dioxide, latent heat, and sensible heat derived from eddy covariance, satellite, and meteorological observations. Journal of Geophysical Research-Biogeosciences, 116, 16. https://doi.org/10.1029/2010jg001566

Kanniah KD, Beringer J, Hutley LB (2010) The comparative role of key environmental factors in determining savanna productivity and carbon fluxes: A review, with special reference to northern Australia. Progress in Physical Geography, 34(4), 459-490. https://doi.org/10.1177/0309133310364933

Kanniah KD, Beringer J, Hutley LB (2013) Response of savanna gross primary productivity to interannual variability in rainfall: Results of a remote sensing based light use efficiency model. Progress in Physical Geography-Earth and Environment, 37(5), 642-663. https://doi.org/10.1177/0309133313490006

Keenan TF, Gray J, Friedl MA *et al.* (2014) Net carbon uptake has increased through warming-induced changes in temperate forest phenology. Nature Climate Change, 4(7), 598-604. https://doi.org/10.1038/nclimate2253

Keith H, Van Gorsel E, Jacobsen KL, Cleugh HA (2012) Dynamics of carbon exchange in a *Eucalyptus* forest in response to interacting disturbance factors. Agricultural and Forest Meteorology, 153, 67-81. https://doi.org/10.1016/j.agrformet.2011.07.019

Kirschbaum MUF, Keith H, Leuning R, Cleugh HA, Jacobsen KL, Van Gorsel E, Raison RJ (2007) Modelling net ecosystem carbon and water exchange of a temperate *Eucalyptus delegatensis* forest using multiple constraints. Agricultural and Forest Meteorology, 145(1-2), 48-68. https://doi.org/10.1016/j.agrformet.2007.04.002

Koenkier R (2019) quantreg: Quantile regression. R package version 5.54. https://CRAN.R-project.org/package=quantreg.

Kumarathunge DP, Medlyn BE, Drake JE *et al.* (2019) Acclimation and adaptation components of the temperature dependence of plant photosynthesis at the global scale. New Phytologist, 222(2), 768-784. https://doi.org/10.1111/nph.15668

Lawlor DW (1995) The effects of water deficit on photosynthesis. In: *Environment and Plant Metabolism: Flexibility and Acclimation.* (ed Smirnoff N) pp 129-160. Oxford, Bios Scientific Publishers Ltd.

Leuning R (1995) A critical-appraisal of a combined stomatal-photosynthesis model for C-3 plants. Plant Cell and Environment, 18(4), 339-355. https://doi.org/10.1111/j.1365-3040.1995.tb00370.x

Liu YW (2020) Optimum temperature for photosynthesis: from leaf- to ecosystem-scale. Science Bulletin, 65(8), 601-604. https://doi.org/10.1016/j.scib.2020.01.006

Longstreth DJ, Nobel PS (1980) Nutrient influences on leaf photosynthesis - effects of nitrogen, phosphorus, and potassium for *Gossypium hirsutum l*. Plant Physiology, 65(3), 541-543. https://doi.org/10.1104/pp.65.3.541

Ludlow MM, Wilson GL (1971) Photosynthesis of tropical pasture plants .1. Illuminance, carbon dioxide concentration, leaf temperature, and leaf-air vapour pressure difference. Australian Journal of Biological Sciences, 24(3), 449-&.

Luo YQ, Keenan TF, Smith M (2015) Predictability of the terrestrial carbon cycle. Global Change Biology, 21(5), 1737-1751. https://doi.org/10.1111/gcb.12766

Ma SY, Osuna JL, Verfaillie J, Baldocchi DD (2017) Photosynthetic responses to temperature across leaf-canopy-ecosystem scales: a 15-year study in a Californian

oak-grass savanna. Photosynthesis Research, 132(3), 277-291. https://doi.org/10.1007/s11120-017-0388-5

Ma XL, Huete A, Moore CE *et al.* (2020) Spatiotemporal partitioning of savanna plant functional type productivity along NATT. Remote Sensing of Environment, 246, 17. 10.1016/j.rse.2020.111855

Malhi Y, Girardin CaJ, Goldsmith GR *et al.* (2017) The variation of productivity and its allocation along a tropical elevation gradient: A whole carbon budget perspective. New Phytologist, 214(3), 1019-1032. https://doi.org/10.1111/nph.14189

Mau AC, Reed SC, Wood TE, Cavaleri MA (2018) Temperate and tropical forest canopies are already functioning beyond their thermal thresholds for photosynthesis. Forests, 9(1), 24. https://doi.org/10.3390/f9010047

Moore CE, Beringer J, Donohue RJ, Evans B, Exbrayat JF, Hutley LB, Tapper NJ (2018) Seasonal, interannual and decadal drivers of tree and grass productivity in an Australian tropical savanna. Global Change Biology, 24(6), 2530-2544. https://doi.org/10.1111/gcb.14072

Moore CE, Beringer J, Evans B, Hutley LB, Mchugh I, Tapper NJ (2016) The contribution of trees and grasses to productivity of an Australian tropical savanna. Biogeosciences, 13(8), 2387-2403. https://doi.org/10.5194/bg-13-2387-2016

Moore CE, Beringer J, Evans B, Hutley LB, Tapper NJ (2017) Tree–grass phenology information improves light use efficiency modelling of gross primary productivity for an Australian tropical savanna. Biogeosciences, 14(1), 111-129. https://doi.org/10.5194/bg-14-111-2017

Nakamura A, Kitching RL, Cao M *et al.* (2017) Forests and their canopies: Achievements and horizons in canopy science. Trends in Ecology & Evolution, 32(6), 438-451. https://doi.org/10.1016/j.tree.2017.02.020

Nemani RR, Keeling CD, Hashimoto H *et al.* (2003) Climate-driven increases in global terrestrial net primary production from 1982 to 1999. Science, 300(5625), 1560-1563. https://doi.org/10.1126/science.1082750

Niu SL, Luo YQ, Fei SF *et al.* (2012) Thermal optimality of net ecosystem exchange of carbon dioxide and underlying mechanisms. New Phytologist, 194(3), 775-783. https://doi.org/10.1111/j.1469-8137.2012.04095.x

Pau S, Detto M, Kim Y, Still CJ (2018) Tropical forest temperature thresholds for gross primary productivity. Ecosphere, 9(7), 12. https://doi.org/10.1002/ecs2.2311

R Core Team (2017) *R: A language and environment for statistical computing,* Vienna, Austria.

Reichstein M, Falge E, Baldocchi D *et al.* (2005) On the separation of net ecosystem exchange into assimilation and ecosystem respiration: Review and improved algorithm. Global Change Biology, 11(9), 1424-1439. https://doi.org/10.1111/j.1365-2486.2005.001002.x

Renchon AA, Griebel A, Metzen D *et al.* (2018) Upside-down fluxes Down Under: CO_2 net sink in winter and net source in summer in a temperate evergreen broadleaf forest. Biogeosciences, 15(12), 3703-3716. https://doi.org/10.5194/bg-15-3703-2018

Rogers A, Medlyn BE, Dukes JS *et al.* (2017) A roadmap for improving the representation of photosynthesis in Earth system models. New Phytologist, 213(1), 22-42. https://doi.org/10.1111/nph.14283

Sage RF, Kubien DS (2007) The temperature response of C-3 and C-4 photosynthesis. Plant Cell and Environment, 30(9), 1086-1106. https://doi.org/10.1111/j.1365-3040.2007.01682.x

Schimel D, Stephens BB, Fisher JB (2015) Effect of increasing CO_2 on the terrestrial carbon cycle. Proceedings of The National Academy of Sciences of The United States Of America, 112(2), 436-441. https://doi.org/10.1073/pnas.1407302112/-/DCSupplemental

Shirke PA, Pathre UV (2004) Influence of leaf-to-air vapour pressure deficit (VPD) on the biochemistry and physiology of photosynthesis in *Prosopis juliflora*. Journal of Experimental Botany, 55(405), 2111-2120. https://doi.org/10.1093/jxb/erh229

Smith MN, Taylor TC, Van Haren J *et al.* (2020) Empirical evidence for resilience of tropical forest photosynthesis in a warmer world. Nature Plants, 6(10), 1225-1230. https://doi.org/10.1038/s41477-020-00780-2

Song X, Barbour MM, Saurer M, Helliker BR (2011) Examining the large-scale convergence of photosynthesis-weighted tree leaf temperatures through stable oxygen isotope analysis of multiple data sets. New Phytologist, 192(4), 912-924. https://doi.org/10.1111/j.1469-8137.2011.03851.x

Sprintsin M, Chen JM, Desai A, Gough CM (2012) Evaluation of leaf-to-canopy upscaling methodologies against carbon flux data in North America. Journal of Geophysical Research: Biogeosciences, 117(G1). https://doi.org/10.1029/2010jg001407

Stern H, Dahni RR (2013) The distribution of climate zones across Australia: Identifying and explaining changes during the past century. American Meteorological Society. *25th Conference on Climate Variability and Change.* (pp.

Tern Ozflux (2020, 17 February) *Ozflux monitoring sites*. TERN. ozflux.org.au/monitoringsites/

Valladares F, Laanisto L, Niinemets Ü, Zavala MA (2016) Shedding light on shade: Ecological perspectives of understorey plant life. Plant Ecology & Diversity*,* 9(3), 237-251. https://doi.org/10.1080/17550874.2016.1210262

Vico G, Way DA, Hurry V, Manzoni S (2019) Can leaf net photosynthesis acclimate to rising and more variable temperatures? Plant Cell and Environment*,* 42(6), 1913-1928. https://doi.org/10.1111/pce.13525

Vitousek PM, Porder S, Houlton BZ, Chadwick OA (2010) Terrestrial phosphorus limitation: Mechanisms, implications, and nitrogen-phosphorus interactions. Ecological Applications*,* 20(1), 5-15. https://doi.org/10.1890/08-0127.1

Way DA (2019) Just the right temperature. Nature Ecology & Evolution*,* 3(5), 718-719. https://doi.org/10.1038/s41559-019-0877-3

Webb RA (1972) Use of the Boundary Line in the analysis of biological data. Journal of Horticultural Science*,* 47(3), 309-319. https://doi.org/10.1080/00221589.1972.11514472

Whitley RJ, Macinnis-Ng CMO, Hutley LB *et al.* (2011) Is productivity of mesic savannas light limited or water limited? Results of a simulation study. Global Change Biology*,* 17(10), 3130-3149. https://doi.org/10.1111/j.1365-2486.2011.02425.x

Williams RJ, Myers BA, Muller WJ, Duff GA, Eamus D (1997) Leaf phenology of woody species in a North Australian tropical savanna. Ecology*,* 78(8), 2542-2558.

Wilson KB, Baldocchi DD, Hanson PJ (2000) Spatial and seasonal variability of photosynthetic parameters and their relationship to leaf nitrogen in a deciduous forest. Tree Physiology*,* 20(9), 565-578.

Wilson KB, Baldocchi DD, Hanson PJ (2001) Leaf age affects the seasonal pattern of photosynthetic capacity and net ecosystem exchange of carbon in a deciduous forest. Plant Cell and Environment*,* 24(6), 571-583. https://doi.org/10.1046/j.0016-8025.2001.00706.x

Woodgate W, Van Gorsel E, Hughes D, Suarez L, Jimenez-Berni J, Held A (2020) THEMS: An automated thermal and hyperspectral proximal sensing system for canopy

reflectance, radiance and temperature. Plant Methods, 16(1), 105. https://doi.org/10.1186/s13007-020-00646-w

Wright TE, Tausz M, Kasel S, Volkova L, Merchant A, Bennett LT (2012) Edge type affects leaf-level water relations and estimated transpiration of *Eucalyptus arenacea*. Tree Physiology, 32(3), 280-293. https://doi.org/10.1093/treephys/tps001

Wu J, Albert LP, Lopes AP *et al.* (2016) Leaf development and demography explain photosynthetic seasonality in Amazon evergreen forests. Science, 351(6276), 972-976. https://doi.org/10.1126/science.aad5068

Wu J, Guan KY, Hayek M *et al.* (2017) Partitioning controls on Amazon forest photosynthesis between environmental and biotic factors at hourly to interannual timescales. Global Change Biology, 23(3), 1240-1257. https://doi.org/10.1111/gcb.13509

Yamori W, Hikosaka K, Way DA (2014) Temperature response of photosynthesis in C-3, C-4, and CAM plants: Temperature acclimation and temperature adaptation. Photosynthesis Research, 119(1-2), 101-117. https://doi.org/10.1007/s11120-013-9874-6

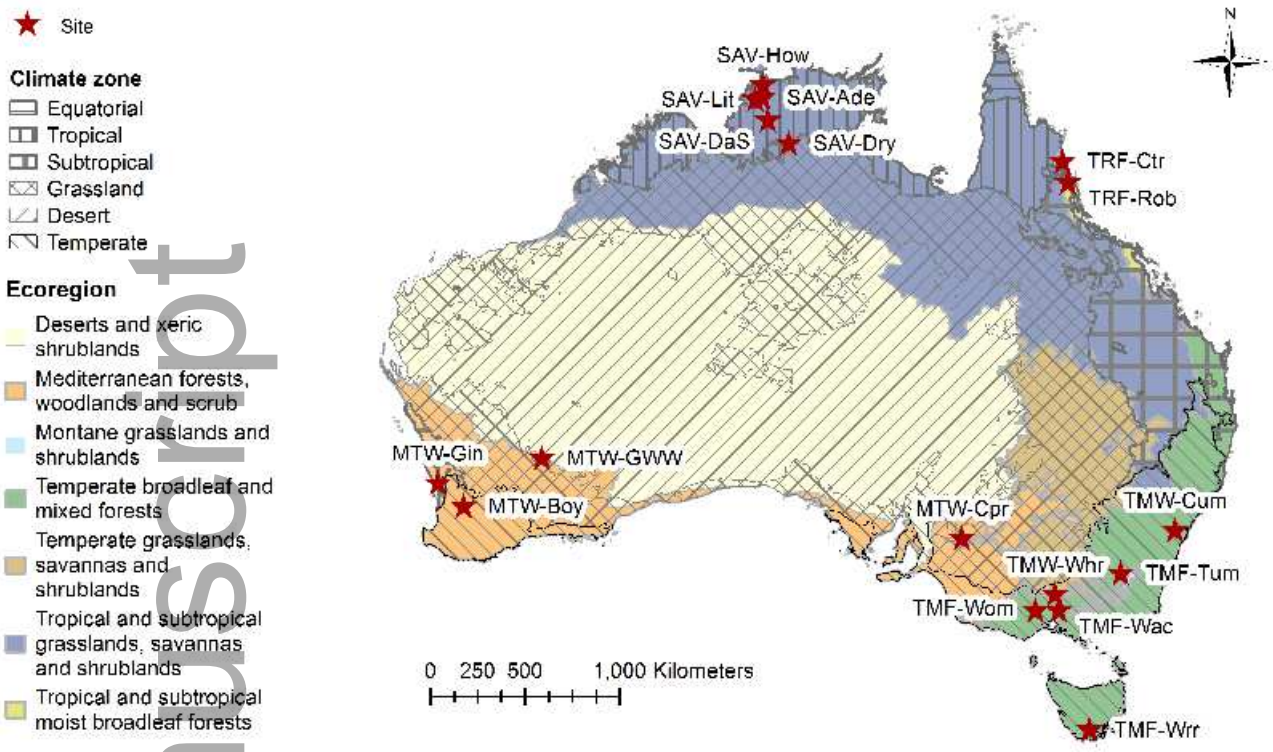

gcb_15760_f1.jpg

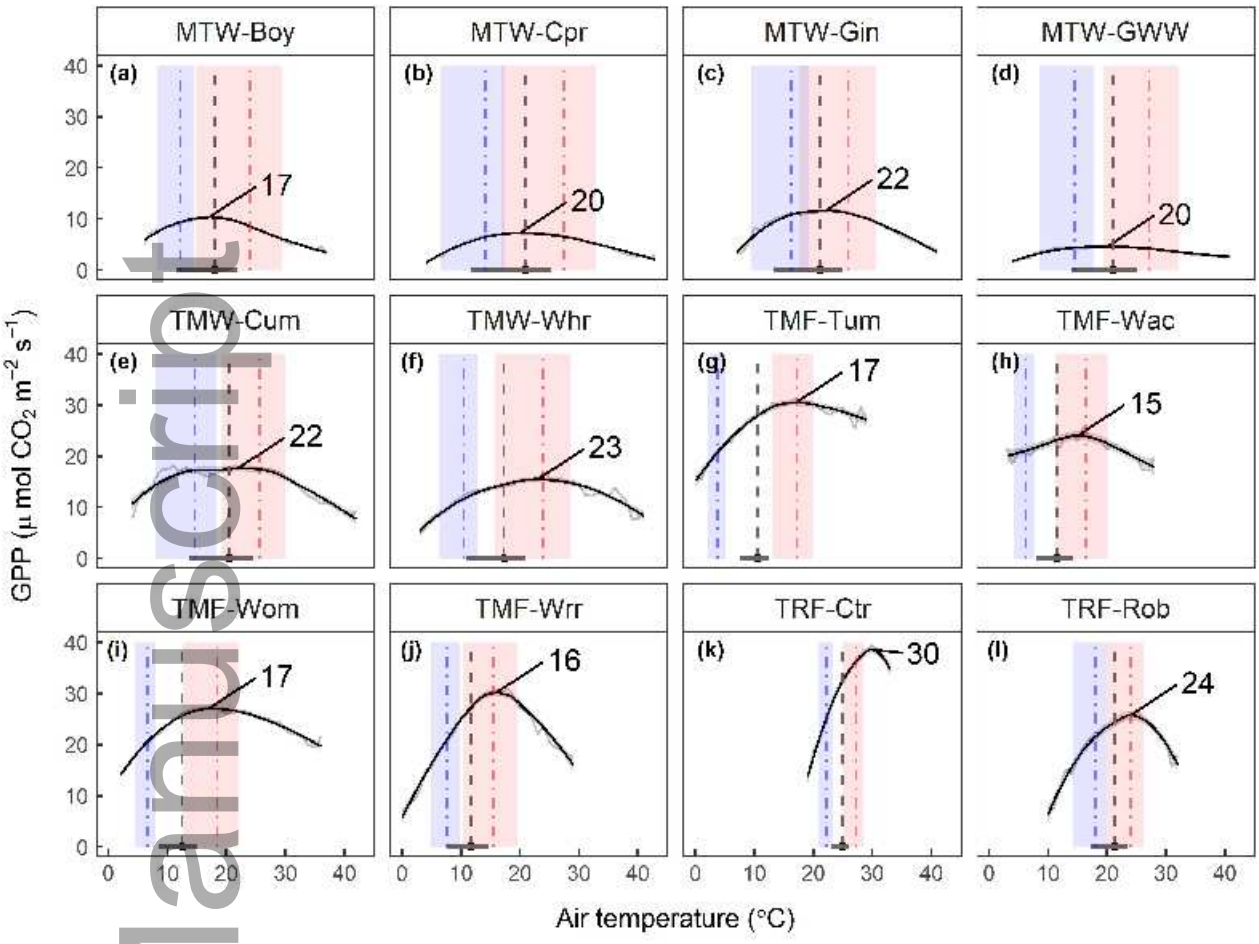

gcb_15760_f2.jpg

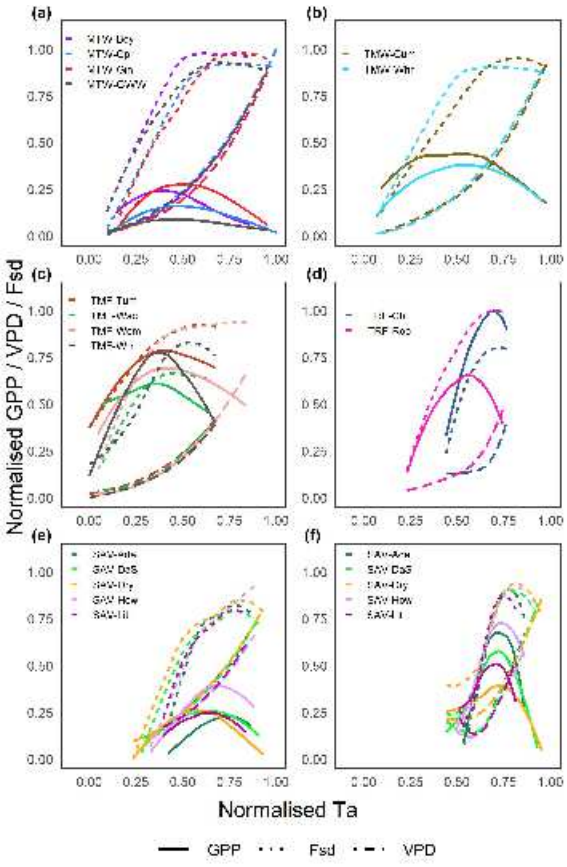

gcb_15760_f3.jpg

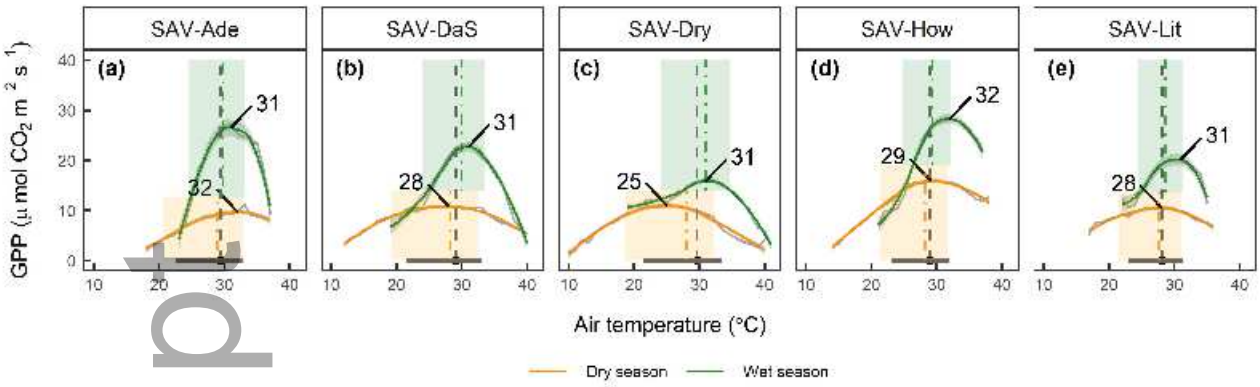

gcb_15760_f4.jpg

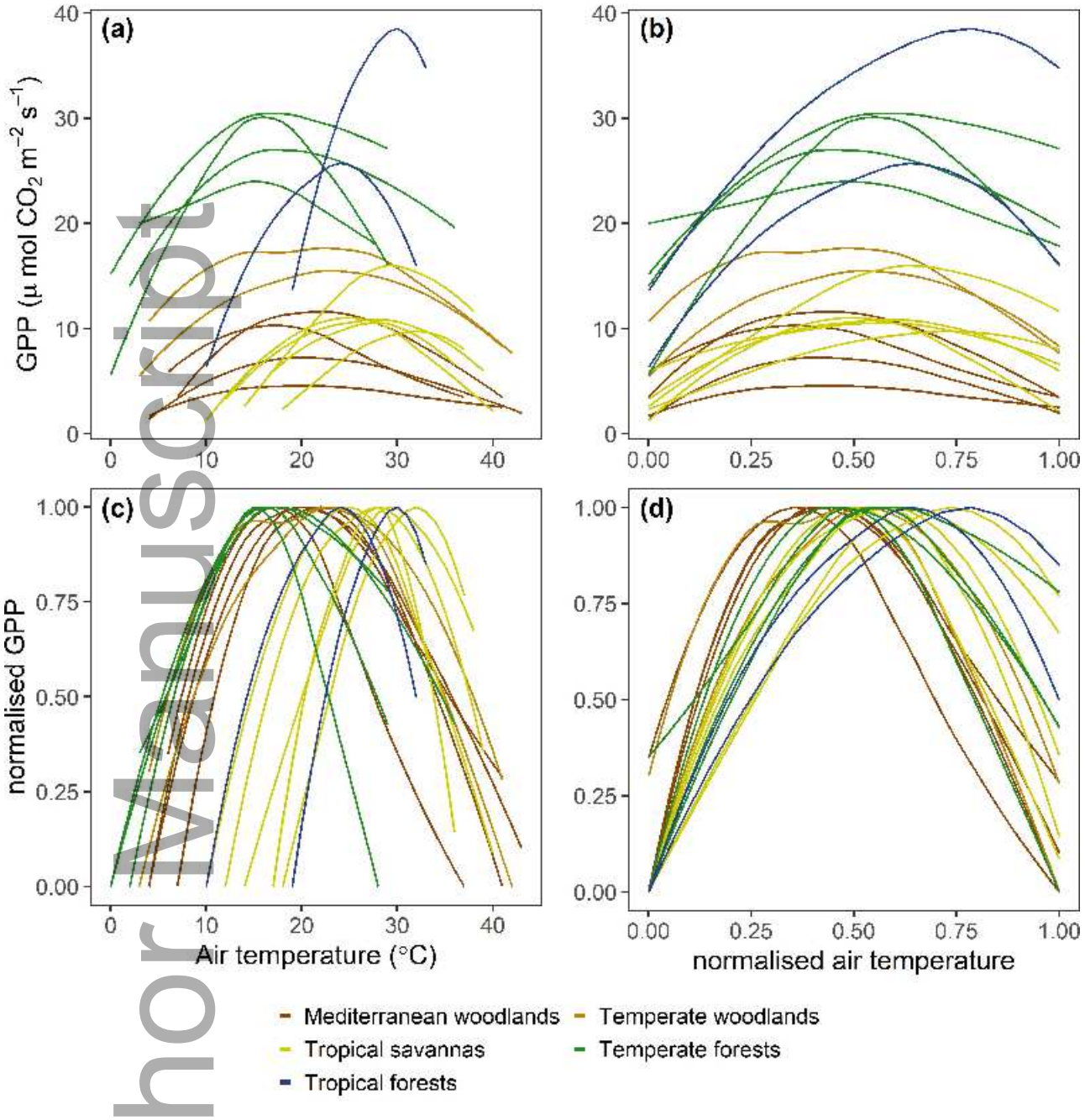

gcb_15760_f5.jpg

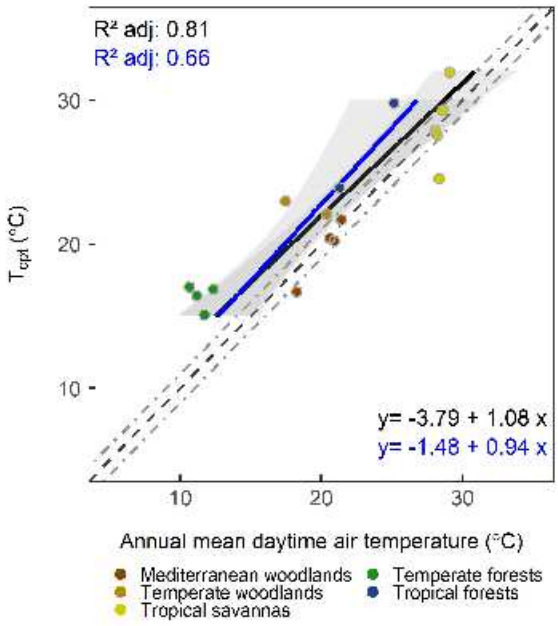

gcb_15760_f6.jpg